Measurements of Deuteron Threshold Electrodisintegration: A Probe of Short-Range Meson Exchange

K. S. Lee,[1] W. Schmitt,[2] H. Baghaei,[1],[a] D. Beck,[5] P. E. Bosted,[3] S. Churchwell,[1] B. Frois,[4] R. S. Hicks,[1] A. Hotta,[6] J. Martino,[4] R. A. Miskimen,[1] G. A. Peterson,[1] S. Platchkov,[4] M. Spengos,[3] W. Turchinetz,[2] K. Wang,[1] C. F. Williamson,[2] T. Yates,[2] and J. D. Zumbro[2]

[1]*University of Massachusetts, Amherst, Massachusetts 01003*
[2]*Massachusetts Institute of Technology, Cambridge, Massachusetts 02139*
[3]*The American University, Washington, D.C. 20016*
[4]*Centre d'Études Nucléaires de Saclay, F-91191 Gif-sur-Yvette, France*
[5]*University of Illinois, Champaign, Illinois 61820*
[6]*Shizuoka University, Shizuoka 422, Japan*

(Received 25 July 1991)

The threshold electrodisintegration of the deuteron was measured with good energy resolution to a maximum four-momentum transfer squared of 42 fm^{-2}. The data are compared with meson exchange calculations that show sensitivity to the choice of exchange-current form factor, the nucleon electromagnetio form factors, and the nucleon-nucleon potential. While conventional theories can give a reasonable description of the data, comparison of the data with quark cluster calculations shows poor agreement.

PACS numbers: 25.30.Dh, 21.30.+y, 25.10.+s, 27.10.+h

In conventional models, the nucleon-nucleon force is mediated by meson exchange. One of the most striking examples for the validity of the meson exchange representation of the nucleon-nucleon (NN) force is found in the threshold electrodisintegration of the deuteron at backward electron-scattering angles [1-3]. At low excitation energy in the neutron-proton center of mass (E_{np}), this reaction is dominated by an $M1$ spin-flip transition between the deuteron ground state and the unbound $^1S_0$ $T=1$ scattering state. At a four-momentum transfer squared (Q^2) of approximately 12 fm^{-2}, the consideration of meson exchange currents (MEC) is essential in explaining the absence of a minimum predicted to exist in the cross section due to the destructive interference between $^3S_1 \rightarrow {}^1S_0$ and $^3D_1 \rightarrow {}^1S_0$ transitions [4].

At higher momentum transfers, where Q^2 equals or exceeds M_N^2, the reaction becomes sensitive to factors that include relativistic effects, the NN potential model, and the nucleon electromagnetic (EM) form factors [5]. The availability of data at high Q^2 not only serves as a test of these effects, but also probes MEC with a spatial resolution where mesonic theories may no longer be valid. In particular, for $Q^2 > 40$ fm^{-2} the spatial resolution of the photon probe is less than the typical hadronic size of 1 fm. Indeed, several exploratory calculations have been made of threshold electrodisintegration which treat the deuteron as a six-quark cluster at short distances. As the simplest nucleus, the deuteron can provide the most unambiguous test of such concepts.

Previous measurements of the threshold electrodisintegration lack either the Q^2 range or the energy resolution required to comprehensively examine non-nucleonic effects in the kinematic region where these are expected to be dominant. Data [1,2] from Saclay have good resolution, $\Delta E_{np}=1.7$ MeV full width at half maximum (FWHM), but only extend to $Q^2=28$ fm^{-2}. Data [3] from SLAC extend to $Q^2=71$ fm^{-2} but have coarse resolution, $\Delta E_{np}=10$-20 MeV FWHM. Coarse resolution complicates the interpretation of the data and may obscure features such as the possible presence of a minimum in the differential cross section near threshold. Moreover, the theoretical calculations predict considerably different shapes for the differential cross section; some models predict cross sections that rise monotonically with E_{np} and others give sharp cusps just above threshold [3]. Such features cannot be resolved in poor resolution experiments.

In this Letter new measurements are presented for the threshold electrodisintegration of the deuteron at high Q^2 with good energy resolution, $\Delta E_{np} \approx 2.5$ MeV FWHM. The experiment was performed at the MIT Bates Linear Accelerator using the Energy Loss Spectrometer System [6]. Data were taken at beam energies of 347, 574, 750, 813, and 903 MeV at a scattering angle of 160°, corresponding to momentum transfers of 8.7, 20.5, 31.3, 35.5, and 41.7 fm^{-2}, respectively. The liquid deuterium (LD_2) target cell [7], constructed from 0.94-mm-thick aluminum, was approximately 10 cm long in the beam direction and 2 cm wide in the transverse direction. Because the cell was not movable, only LD_2 was normally available for data taking. Slits near the target cell defined an effective target length of 3.6 cm. The solid-angle defining slits in front of the spectrometer were adjusted to give the maximum usable solid angle of approximately 3.7 msr.

Because the anticipated count rate at the highest Q^2 was only a few counts per day, the spectrometer focal plane and data acquisition software were optimized for background rejection. Drift chambers in the spectrometer focal plane were used to restrict the range of acceptable track angles, greatly reducing cosmic-ray backgrounds. The remaining cosmic-ray muons were rejected with a 12-radiation-length lead-glass shower-counter ar-

ray. Pions were rejected with a Čerenkov counter that used isobutane at atmospheric pressure as the light-producing medium. The observed pulse-height distribution was consistent with the detection of seven photoelectrons per incident electron. Electron backgrounds due to the scattering of the beam halo from the target cell walls were negligible.

To verify the observed position of the deuteron elastic peak, $d(e,\pi^-)pp$ data were taken near the kinematic end-point region of this reaction. At 903 MeV an additional measurement was made of hydrogen elastic scattering. These data were used to predict the position in the focal plane of the deuteron elastic peak relative to the positions of the (e,π^-) end point and the hydrogen elastic peak. The results of this calibration are nearly independent of beam energy uncertainties. In all cases, the elastic peak predictions agreed with the observed peak positions to within $\Delta E_{np} = \pm 1$ MeV.

The beam energy uncertainties are estimated to be less than $\pm 0.6\%$. For the 750- and 813-MeV data, the beam energy was inferred from the position of the deuterium elastic peak using a focal plane calibration based on known beam energies [8] for the 347- and 574-MeV data. For the 903-MeV data, the beam energy was obtained by measuring the recoil energy difference between elastic hydrogen and deuterium scattering. The result of the recoil energy analysis agreed with the value based upon the focal plane calibration.

Radiative corrections to the data were assessed for each value of E_{np} by means of a Monte Carlo simulation [9] that included Landau straggling and bremsstrahlung [10]. In no case did the calculated elastic radiation tail exceed 23% of the cross section observed near threshold.

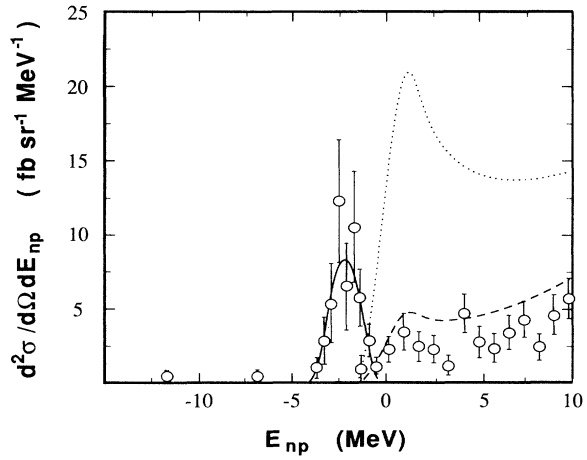

FIG. 1. Threshold electrodisintegration cross sections as a function of E_{np} at 750 MeV. The solid curve is the Monte Carlo resolution function. Paris potential calculations [5], using dipole EM form factors and folded with the Monte Carlo resolution, are also shown: The dotted and dashed curves are with G_E^V and F_1^V exchange-current form factors, respectively.

Figure 1 shows the 750-MeV cross sections corrected for radiative effects as a function of E_{np}. The resolution function resulting from the Monte Carlo and normalized to the same elastic cross section is also shown. The systematic errors in the cross sections, estimated at approximately $\pm 5\%$ and dominated by uncertainties in target thickness and density, are negligible compared to the statistical errors for all but the 347-MeV data point. The elastic-scattering data are in agreement with previously measured values for the deuterium elastic cross section [11] at 347 MeV and the hydrogen elastic cross section [12] at 903 MeV.

Figure 2 shows the Q^2 dependence of the threshold data averaged over the range $E_{np}=0$–3 MeV, along with previous results [1,2] from Saclay that had comparable energy resolution. Figure 3 compares these data sets with coarse resolution data [3] from SLAC that were averaged over a range $E_{np}=0$–10 MeV. The new data presented here show that the cross section departs from a pure exponential slope at $Q^2 \approx 25$ fm^{-2}. Furthermore, no evidence is observed for a diffraction minimum in this momentum-transfer region.

Calculations by Singh, Leidemann, and Arenhövel [5] and Schiavilla and Riska [13] are shown in Figs. 2 and 3, respectively. These nonrelativistic calculations are similar in that they use a current operator that is consistent with the interaction model [14]. Singh, Leidemann, and Arenhövel use the Paris potential [15] and sum over all

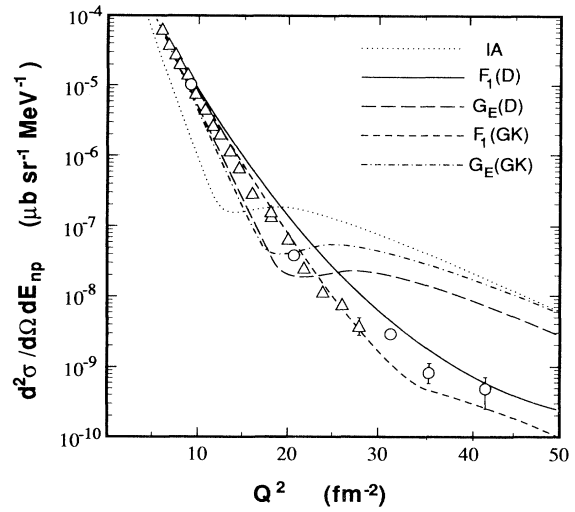

FIG. 2. Threshold electrodisintegration cross sections averaged over $E_{np}=0$–3 MeV compared with Paris potential calculations [5]. The open circles represent data from this measurement; the triangles represent data from Saclay [1,2]. The dotted curve is the impulse approximation (IA), the solid curve is for F_1^V and dipole nucleon EM form factors, the long-dashed curve is for G_E^V and dipole form factors, the short-dashed curve is for F_1^V and GK [17] form factors, and the dash-dotted curve is for G_E^V and GK form factors. The calculations are evaluated at $E_{np}=1.5$ MeV.

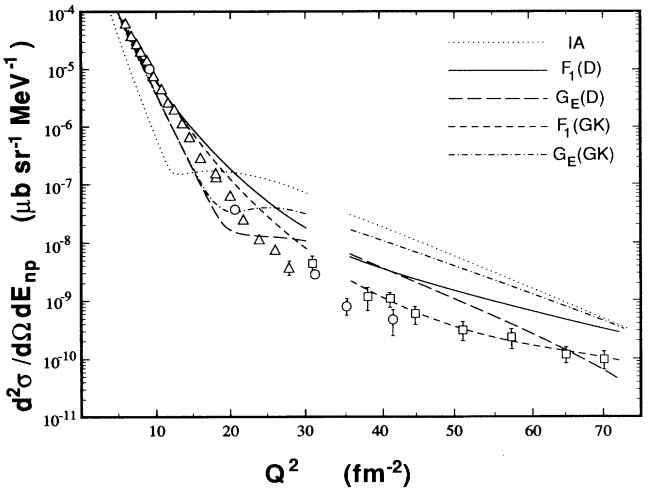

FIG. 3. Same as for Fig. 2 except that the calculations [13] use the Argonne v_{14} potential. The squares represent data from SLAC averaged over $E_{np}=0$–10 MeV [3]. The break in the theory curves indicate an average over $E_{np}=0$–3 MeV for $Q^2<32$ fm^{-2} and over $E_{np}=0$–10 MeV for $Q^2>32$ fm^{-2}.

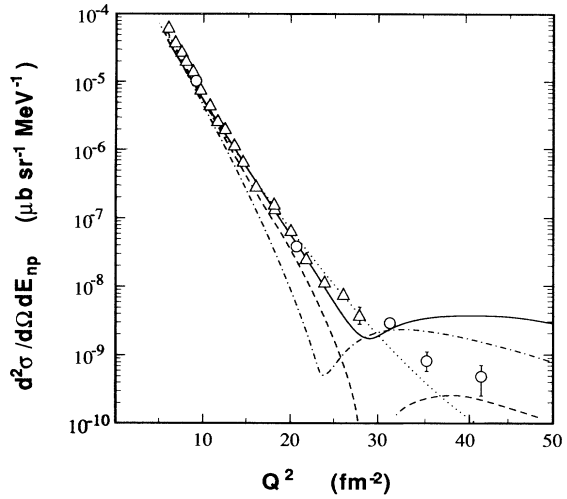

FIG. 4. Threshold electrodisintegration cross sections compared with meson exchange and quark cluster calculations. The dashed curve is a calculation by Truhlik and Adam [20] for standard MEC (impulse approximation $+\pi+\rho$), and the dotted curve is their calculation for standard MEC including nonpotential A_1 and heavy-meson currents ($\sigma+\omega+\delta+\eta$). The solid and dash-dotted curves are quark cluster calculations by Cheng and Kisslinger [22] and Yamauchi, Buchmann, and Faessler [23], respectively. The calculations are evaluated at $E_{np}=1.5$ MeV.

partial waves up to $L=4$ in the n-p scattering state. Schiavilla and Riska use the Argonne v_{14} potential [16] and sum over all partial waves up to $J\leq 2$. To ensure current conservation, both calculations use the isovector nucleon EM form factor to describe the structure of the MEC. In these calculations there is an ambiguity as to whether the isovector Dirac (F_1^V) or the isovector Sachs form factor (G_E^V) should be used for the exchange current. Figure 2 shows Paris potential results for both F_1^V and G_E^V for the exchange current, as well as for nucleon EM form factors given by either the dipole or the Gari and Krümpelmann [17] (GK) expression. Figure 3 shows corresponding results for the Argonne v_{14} potential. This approach differs from that of Gross and co-workers [18], who have shown that a single universal form factor, such as F_1^V or G_E^V, is not required by current conservation and that a conserved current can be constructed using different EM form factors for the pion, nucleon, and contact contributions.

The theoretical results shown in Figs. 2 and 3 demonstrate the strong effect of MEC in this reaction. Below $Q^2\approx 15$ fm^{-2} MEC give larger cross sections than obtained in the IA result; above 15 fm^{-2} MEC decrease the cross section by more than an order of magnitude. At high Q^2 the calculations show a strong sensitivity to the choice of the exchange-current form factor. The use of G_E^V in the form factor produces a minimum in the cross section that is not manifest in the data. In comparison, a smooth decrease is obtained with F_1^V, which corresponds more closely to the data. This behavior is potential dependent, and results obtained with the Bonn potentials show better agreement with data using G_E^V rather than F_1^V [19]. This is attributed to differences between the Paris and v_{14} potentials and the Bonn potential for the predicted D-state admixture in the deuteron and for the radial forms of the S and D waves. The calculations also show sensitivity to the choice of the nucleon EM form factors. For the v_{14} calculation the deviation between the dipole and GK predictions is as great as that between predictions using F_1^V and G_E^V. This is caused primarily by the large difference in the dipole and GK parametrizations of the neutron electric form factor.

Paris potential calculations, folded with the Monte Carlo resolution, are compared with the 750-MeV data as a function of E_{np} in Fig. 1. These calculations use dipole EM form factors, and are given for both F_1^V and G_E^V in the exchange-current form factor. The calculations and data show the persistence of the threshold cusp that has been widely observed [1,2] at much lower values of Q^2. The calculation using F_1^V, besides giving a threshold cross section closer to the data than the calculation using G_E^V, also gives a better representation of the E_{np} dependence of the data.

Truhlik and Adam [20] have calculated deuteron electrodisintegration including the nonpotential $A_1(1^+)$ current and heavy-meson exchange ($\sigma+\omega+\delta+\eta$) using the Bonn OBEPQC potential [21]. Their results are shown in Fig. 4 for standard MEC (impulse approximation $+\pi+\rho$), and for standard MEC including A_1 and heavy meson currents. Only the $M1$ transition amplitude is included in the calculations, and GK and F_1^V are used for the nucleon EM and exchange-current form factors, re-

spectively. The calculations show that the nonpotential and heavy-meson currents have a strong effect at high Q^2. These currents eliminate the minimum in the standard MEC calculation at $Q^2 \approx 30$ fm^{-2}, giving a result that more closely corresponds to the data.

The results of quark cluster calculations by Cheng and Kisslinger [22] and by Yamauchi, Buchmann, and Faessler [23] are also shown in Fig. 4. In Cheng and Kisslinger's model the deuteron is treated as a six-quark state within a 1-fm matching radius and as a two-baryon state outside the radius. Yamauchi, Buchmann, and Faessler use resonating group methods to connect the short-distance six-quark configuration of the deuteron smoothly with the long-distance two-nucleon configuration. These models incorporate not only quark- and gluon-exchange mechanisms at short distance but also MEC at long and intermediate distances. Figure 4 shows that both of these calculations predict a second maximum in the cross section, a feature not observed in the data. While other quark cluster calculations, such as those by Chemtob and Furui [24] and Glozman *et al.* [25], may not show a second maximum, in Cheng and Kisslinger's model this structure cannot be avoided.

In conclusion, these data show that the deuteron threshold electrodisintegration cross section departs from a pure exponential slope at $Q^2 \approx 25$ fm^{-2}, with no evidence for a second maximum at momentum transfers above 25 fm^{-2}. At $Q^2 = 31.3$ fm^{-2} the data show the persistence of the threshold cusp that has been widely observed at much lower values of Q^2. Two advances are required for better understanding of this fundamental $M1$ spin-flip transition in the deuteron: first, a reliable estimate of relativistic effects; and second, accurate experimental data for the electric and magnetic form factors of the proton and neutron. When these form factors are better established, the data presented here will provide an important test for relativistic theories and for models of the NN interaction. Even with spatial resolutions of less than 1 fm, there is no evidence for the breakdown of nucleon-meson theories and no explicit evidence that quark degrees of freedom play a significant role in this Q^2 range.

This work was supported by Department of Energy Grant No. DE-FG02-ER40415 and Contract No. DE-AC02-ER03069, and by National Science Foundation Grant No. 87-15050. We thank H. Arenhövel, R. Schiavilla, and E. Truhlik for communicating the results of their calculations; K. Dow and P. Dunn for their assistance; and CEBAF for supplying phototubes. A.H. acknowledges the support of the Monbusho International Research Program and the Saito Science Foundation.

[a]Present address: University of Virginia, Charlottesville, VA 22901.

[1] M. Bernheim *et al.*, Phys. Rev. Lett. **46**, 402 (1981).
[2] S. Auffret *et al.*, Phys. Rev. Lett. **55**, 1362 (1985).
[3] R. G. Arnold *et al.*, Phys. Rev. C **42**, 1 (1990).
[4] J. Hockert, D. O. Riska, M. Gari, and A. Huffman, Nucl. Phys. **A217**, 14 (1973).
[5] S. K. Singh, W. Leidemann, and H. Arenhövel, Z. Phys. A **331**, 509 (1988); and (private communication).
[6] W. Bertozzi, M. V. Hynes, C. P. Sargent, W. Turchinetz, and C. Williamson, Nucl. Instrum. Methods **162**, 211 (1979).
[7] C. F. Williamson, Bates Linear Accelerator Report No. 88-1, 1988 (unpublished).
[8] D. Beck, Ph.D. thesis, Massachusetts Institute of Technology, 1986.
[9] A. T. Katramatou, SLAC Report No. SLAC-NPAS-TN-86-8, 1986 (unpublished).
[10] L. W. Mo and Y. S. Tsai, Rev. Mod. Phys. **41**, 205 (1969).
[11] S. Platchkov *et al.*, Nucl. Phys. **A510**, 740 (1990); R. G. Arnold (private communication).
[12] R. C. Walker *et al.*, Phys. Lett. B **224**, 353 (1989).
[13] R. Schiavilla and D. O. Riska, Phys. Rev. C **43**, 437 (1991); and (private communication).
[14] D. O. Riska, Phys. Scr. **31**, 471 (1985).
[15] M. Lacombe *et al.*, Phys. Rev. C **21**, 861 (1980).
[16] R. B. Wiringa, R. A. Smith, and T. L. Ainsworth, Phys. Rev. C **29**, 1207 (1984).
[17] M. Gari and W. Krümpelmann, Phys. Lett. B **173**, 10 (1986).
[18] Franz Gross and D. O. Riska, Phys. Rev. C **36**, 1928 (1987); Franz Gross and Hartmut Henning, CEBAF Report No. CEBAF-TH-91-03, 1991 (to be published).
[19] W. Leidemann, K.-M. Schmitt, and H. Arenhövel, Phys. Rev. C **42**, 826 (1990).
[20] E. Truhlik and J. Adam, Jr., Nucl. Phys. **A492**, 529 (1989); and (private communication).
[21] R. Machleidt, Adv. Nucl. Phys. **19**, 189 (1989).
[22] T.-S. Cheng and L. S. Kisslinger, Nucl. Phys. **A457**, 602 (1986).
[23] Y. Yamauchi, A. Buchmann, and A. Faessler, Nucl. Phys. **A494**, 401 (1989); and (private communication).
[24] M. Chemtob and S. Furui, Nucl. Phys. **A449**, 683 (1986).
[25] L. Ya. Glozman, N. A. Burkova, E. I. Kuchina, and V.I. Kukulin, Phys. Lett. B **200**, 406 (1988).